Nitrogen-Mediated Carbon Nanotube Growth: Diameter Reduction, Metallicity, Bundle Dispersability, and Bamboo-like Structure Formation

Bobby G. Sumpter,[†,*] Vincent Meunier,[†] José M. Romo-Herrera,[‡] Eduardo Cruz-Silva,[‡] David A. Cullen,[§] Humberto Terrones,[‡] David J. Smith,[§] and Mauricio Terrones[‡]

[†]Computer Science and Mathematic Division and Center for Nanophase Materials Sciences, Oak Ridge National Laboratory, Bethel Valley Road, Oak Ridge, Tennessee 37831, [‡]Advanced Materials Department, IPICyT, Camino a la Presa San Jose 2055, 78216 San Luis Potosi, Mexico, and [§]School of Materials and Department of Physics, Arizona State University, Tempe, Arizona 85287

ABSTRACT Carbon nanotube growth in the presence of nitrogen has been the subject of much experimental scrutiny, sparking intense debate about the role of nitrogen in the formation of diverse structural features, including shortened length, reduced diameters, and bamboo-like multilayered nanotubules. In this paper, the origin of these features is elucidated using a combination of experimental and theoretical techniques, showing that N acts as a surfactant during growth. N doping enhances the formation of smaller diameter tubes. It can also promote tube closure which includes a relatively large amount of N atoms into the tube lattice, leading to bamboo-like structures. Our findings demonstrate that the mechanism is independent of the tube chirality and suggest a simple procedure for controlling the growth of bamboo-like nanotube morphologies.

KEYWORDS: nanotube growth · nitrogen doping · electronic structure · surfactant · bamboo structures

Carbon nanotubes (CNTs), whether single-walled (SWNT) or multi-walled (MWNT), have unparalleled potential for use as advanced materials. This potential is afforded by the inherently superior combination of mechanical, electrical, and thermal properties.[1–3] However, their use as building blocks in nanocomposites[4] and nanoelectronic devices has still not yet been fully realized. This is in part due to a lack of control of the reactivity of the outer CNT walls and of the basic electronic structure. In this regard, considerable research has explored the effect of doping CNTs with various atoms, including Co, P, K, Si, N, B, and O.[5–25] Common wisdom indicates that insertion of different atoms into a nanotube lattice alters its structure and properties. For instance, boron and nitrogen atoms are among the atoms most conveniently used as dopants of CNTs,[20,21,24] since they have atomic sizes similar to that of carbon, a property that provides them with a strong probability of entering into the carbonaceous lattice. While boron doping has been shown to increase the overall length of nanotubes by preventing tube closure for the zigzag geometry,[26] nitrogen doping has been observed to yield short tubes with smaller diameter, and often corrugated or bamboo-like structures.[27–29] In addition, even though the mechanisms governing the structural changes induced by B doping are now rather well understood,[26,30] much less is known about the corresponding effects of N doping on nanotube structures.

The main goal of the present work is to examine the fundamental nature of the structural changes observed for N-doped CNTs. Specifically, producing SWNTs in the presence of active N species gives rise to several distinguishing features. As the N content increases, the diameter of SWNTs decreases and only narrow-diameter tubes are formed. The tube bundles are easier to disperse when compared to their pure carbon counterparts, while doped tubes oxidize more readily than undoped ones. Corrugation within the tube walls is sometimes observed, and the formation of fullerene-like structures could also occur inside the cores of the N-doped SWNTs, a behavior related to the appearance of bamboo-like SWNTs. Finally, the entanglement of the nanotube strands is reduced as the N content is increased.

In this paper, we develop a simple model that is able to account for all of these seemingly independent features and to understand the mechanisms responsible for the

*Address correspondence to sumpterbg@ornl.gov.

Received for review August 3, 2007 and accepted October 18, 2007.

Published online November 30, 2007.
10.1021/nn700143q CCC: $37.00

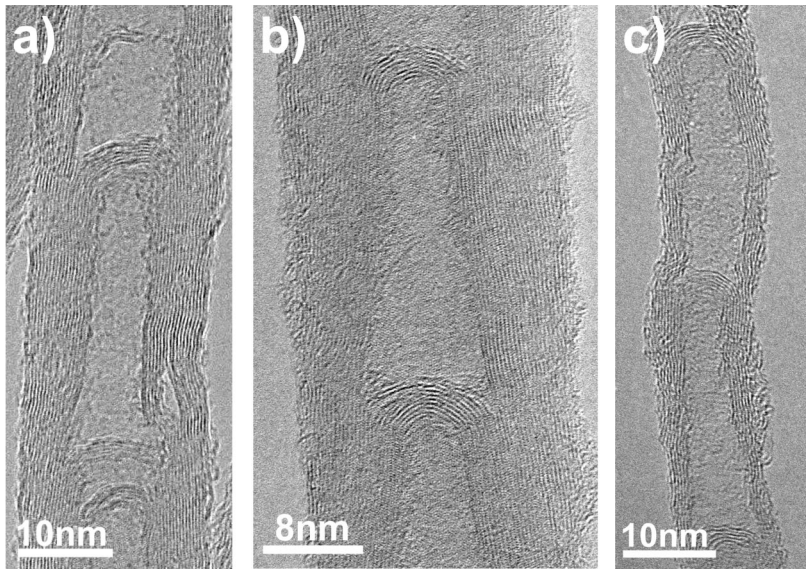

Figure 1. Transmission electron microscopy images of multiwalled carbon nanotubes doped with N atoms, produced by the thermolysis of ferrocene−benzylamine solutions at 850 °C: (a) low-resolution image showing the compartmentalized structure of N-doped MWNTs; (b) high-resolution image of an individual compartment showing the continuous closure of tubes; note that the outer nanotubes sometimes cover the compartments. It has been observed experimentally using elemental line scans that N is richer in the compartment core and on the inner walls of the compartments, indicating that N preferentially sits on narrow-diameter tubes.

structural changes related to N doping. Our model is based on a study consisting of a combination of experimental observations and theoretical calculations. We first report on the synthesis and characterization of N-doped carbon nanotubes and then use results from first-principles static and dynamic calculations within the framework of density functional theory (DFT) to rationalize the observations.

RESULTS AND DISCUSSION

It has been observed that, during the growth of MWNTs, N atoms can lead to the formation of multishell bamboo-like tubular structures or compartmentalized tubules (Figure 1). This is an indication that N atoms cause the creation of pentagons so that positive curvature is induced, resulting in the formation of nanotube caps. In some occasions, these N species form N_2 molecules that can be trapped inside the tubule cores. It is also noteworthy that MWNTs growing in conjunction with N atoms exhibit shorter lengths when compared with MWNTs grown from pure C species.[31] Finally, it has been observed experimentally using elemental line scans that N is richer in the compartment core and on the inner walls of the compartments, indicating that N preferentially sits on narrow-diameter tubes.[32]

From the examination of structural features (see Figure 2) observed by high-resolution transmission electron microscopy (HRTEM), Raman spectroscopy, and thermogravimetric analysis (TGA), one notes several characteristics that arise when SWNTs are produced in the presence of active N species: (i) as the N content increases, the diameter of SWNTs decreases and only narrow-diameter tubes are formed[32] (Figure 2a,c); (ii) the tubes oxidize faster when compared to their pure C counterparts (see also ref 26); (iii) corrugation within the tube walls is sometimes observed (in this case not damaged by the electron beam), and fullerene-like structures are formed inside the cores of the N-doped SWNTs (Figure 2d); (iv) on rare occasions, bamboo-like SWNTs can be observed (see arrows in Figure 2e); (v) the tube bundles appear to be more easily dispersed following sonication treatments (Figure 3) when compared to pure C SWNTs (*e.g.*, N-doped SWNTs disperses faster than pure C SWNTs with 2-propanol as a solvent, the latter requiring twice as long to be dispersed; this is also true for MWNTs); and (vi) the entanglement of the nanotube

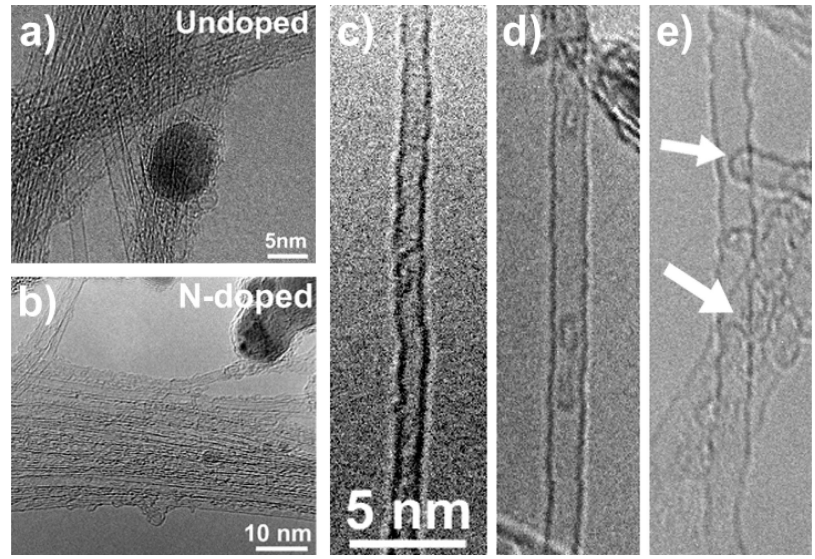

Figure 2. HRTEM images of N-doped SWNTs produced by the pyrolysis at 950 °C of a ferrocene−benzylamine−ethanol solution with a composition ratio of 1.25:7.5:91.25 by weight: (a,b) SWNT bundles showing that N-doped tubes exhibit more compacted bundles of narrow-diameter tubes; (c) N-doped SWNT of narrow diameter (*ca.* 1 nm), exhibiting some degree of corrugation; (d) N-doped SWNT of 1.4 nm diameter, exhibiting fullerene-like structures in its core (possibly N-doped fullerenes that resulted from the frustrated growth of the inner tubules); and (e) highly corrugated N-doped SWNT of large diameter (1.7 nm), exhibiting internal bamboo-like closures (see arrows) as well as a symmetric tubule cap.

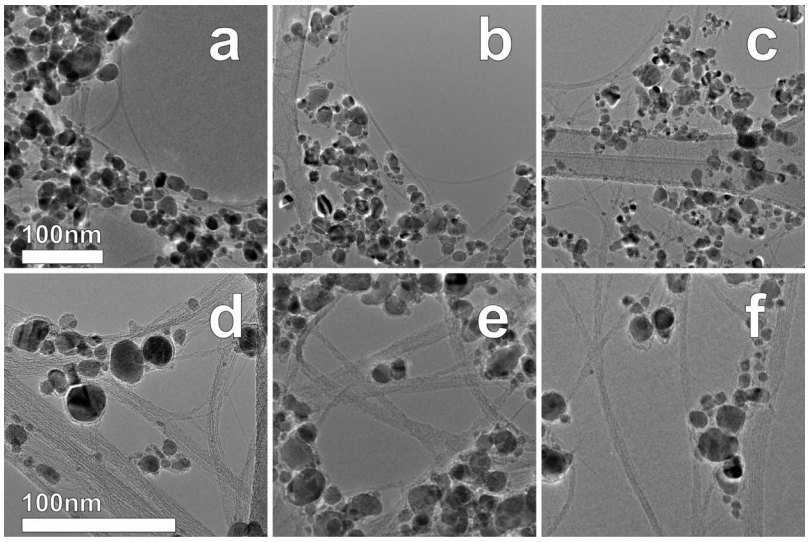

Figure 3. Low-resolution TEM images of SWNTs: (a,d) pristine SWNTs; (b,e) N-doped SWNTs from a solution with 7.5 wt % benzylamine content; and (c,f) N-doped SWNTs from a solution with 15% benzylamine content. As the doping level is increased, the nanotube bundles are smaller and less entangled.

strands is reduced as the N content is increased (see Figure 3).

In order to develop an understanding of the experimental results shown here or published elsewhere, we compared the energetics and dynamics of N-doped zigzag and armchair nanotubes. Each energy point corresponds to a different longitudinal position of a N ring. For comparison, we also considered isolated N atoms (the results for the zigzag tube and single N atoms are in accord with the trends observed for a full ring of N and are not shown). The geometry of the new structure is fully relaxed for each point, and the corresponding energies are summarized in Figure 4. We observe the following features: (1) Nitrogen would rather adsorb (saturate) at the nanotube open end than remain in a molecular state. Note that the reference of energy used here corresponds to an isolated nanotube and nitrogen molecules in the gas phase. Other sources of nitrogen certainly exist in the experiments that have lower binding energies (higher chemical potential) than N_2, and the energetics for N defect formation inside the nanotube bulk can be affected, but saturation at the edge still remains favorable. For N saturation as dangling CN dimers, the formation energy is actually lower by 0.27 eV/N for an (8,0) tube. The stability of edge saturation with dangling CN dimers suggests that carbon feedstock insertion into a N-saturated edge is favorable (a surfactant role for N). Indeed, growth at zigzag nanotube edge that includes N has previously been shown to be significantly enhanced.[33] (2) Nitrogen atoms preferentially substitute at the outer ring at the two-coordinated sites, independent of the chirality (Figure 4). For the zigzag (8,0) tube, this is easy to rationalize since N saturation of the edge removes the eight dangling bonds. We also notice an interesting aspect related to the fact that the armchair edge is favored compared with the zigzag one. However, we note that, in the present case, the effect can at least in part be explained by the relaxed geometry of the CNT end with dangling bonds which reorganize differently in the absence of N atoms. We also note that N saturation at the edge is favorable in part due to the formation of N═N dimers and the elimination of the dangling bonds, a feature that is not possible with single N atom substitution (single atoms can be stable inside the tube).

The fact that nitrogen saturates the nanotube edge ("surfactant" position) suggests some interesting possibilities for its mediating role in the growth of CNTs. First, since N prefers to be at the tube edge and would not be as stable deeper in the hexagonal lattice, its presence could inhibit the growth of the nanotube once the edges are N-saturated. This result is a striking indication of the *surfactant* role of N: the tube cannot grow further unless N is removed and replaced by carbon, or defects are formed. Second, the presence of N on the end tubule is clearly accompanied by a local reduction of the tube diameter at the apex. The tube diameter reduction, expressed in percentage compared to original diameter, for three tubes of varying chiral angles was found to be −6.4%, −3.5%, and −2.2% for (8,0), (9,3), and (6,6) tubes, respectively. In addition, we note that N tends to prefer substitution into smaller diameter tubes, independent of the tube chirality. This clearly indicates that N doping during growth leads to smaller diameter tubes, a fact in strong agreement with experiment (see above).[27]

We also explored how adding N atoms affects tube closure by moving a N ring rigidly between a tube capped end and the tube "bulk". These calculations show that a ring of N prefers to be closer to the end cap than in the bulk, thereby indicating that N slightly favors closure of the tube (see Supporting Information, Figure S1). This supports recent results which demonstrate that nitrogen can stabilize neighboring pentagons in fullerenes isomers.[34] A good surfactant generally facilitates growth by allowing subsurface insertion of the feedstock material at reduced energetic cost. In that respect, nitrogen appears not to be a great surfactant, since we find that it can promote tube closure, leading to shorter tubes. In comparison to boron-mediated nanotube growth,[26] the surfactant effect of N is clearly different. B-doped tubes prefer zigzag edges

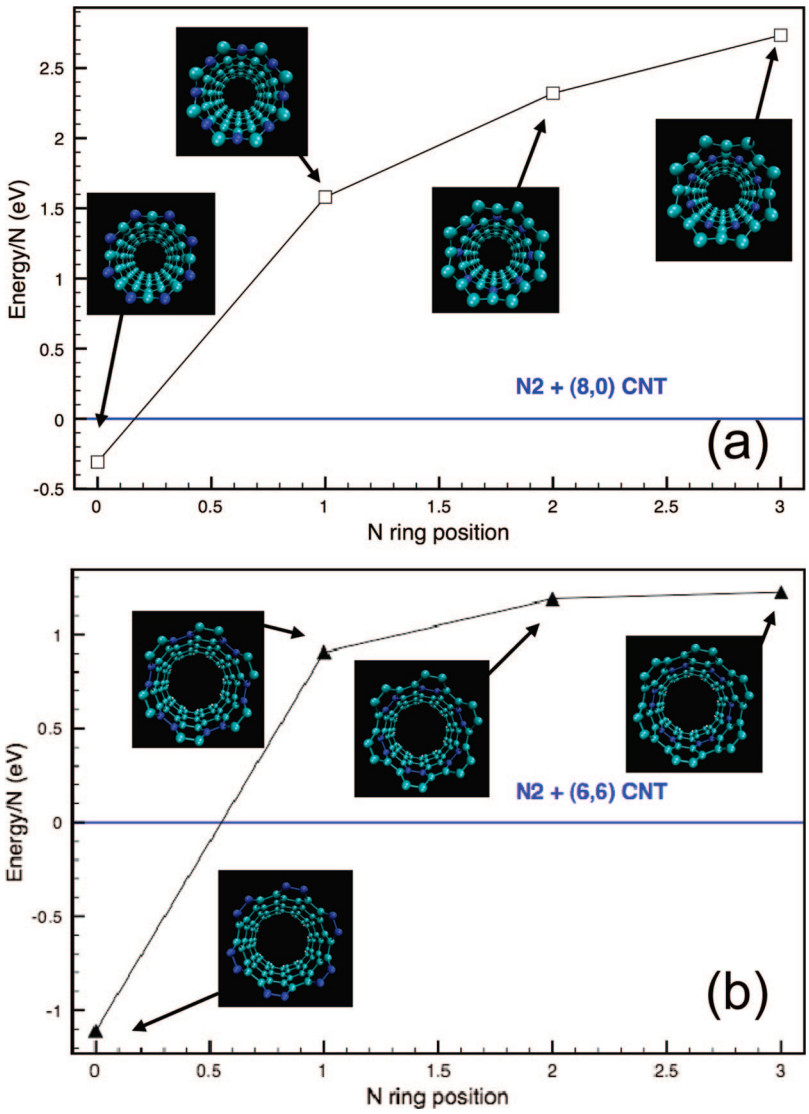

Figure 4. (a) Energetics associated with inserting a full ring, 12 N atoms, at different lattice positions into a cleaved (6,6) SWNT. (b) Energetics associated with inserting a full ring, 8 N atoms, at different lattice positions into a cleaved (8,0) SWNT.

and close at very long times, even if pentagons are formed on the growing edge. For N-doped tubes the armchair edges are preferred, and as pentagons are formed, some curvature is achieved, causing the tubes to begin closing. However, as more N atoms come, the tube must reopen and start growing, resulting in bamboo-like or corrugated configurations. Although both B and N act as surfactants, for N this can lead to the formation of bamboo structures and for B to grow longer. Overall, the results of our investigations unequivocally point to the fact that the presence of N during growth promotes reduction of the tube diameter which will eventually lead to the tube closure (fast creation of pentagons such as the bamboo morphologies).

In order to better understand the role of the surfactant N atoms in the dynamical behavior at temperatures relevant to synthesis, first-principles molecular dynamics in the canonical ensemble were performed. Starting with the ideal open (8,0) undoped SWNT, the temperature was increased to 2500 K and the dynamics followed for 5 ps. The results show the expected behavior of rapid formation of pentagons (pentagons form within 1 ps, notable in the decreased diameter, and persist throughout the entire simulation) at the growing rim, which results in the subsequent partial inward collapsing of the edge structure, leading to a defected graphitic dome and partial closure of the tubule. Figure 5 shows snapshots of the dynamics and the time dependence of the average tube rim diameter when N atoms are substituted at the 2-coordinated sites of the tube rim. After 4 ps of dynamics at 2500 K, no stable pentagons have formed at the edge, and those which did form during the simulation as a result of an atomic N−N bridge across the tube end (t = 0.163 ps) were relatively short-lived (<0.1 ps). Also, N-substitution clearly causes a decrease in the local diameter. HR-TEM images and Raman spectroscopy indicate that, as the N content is increased in the starting solution that is thermally decomposed, the growth of large-diameter tubes is inhibited. This suggests the N atoms remain included in the nanotube lattice, and indeed conductivity measurements support this argument.[27] However, as discussed above, according to static calculations, the addition of a closed cap to the rim of a N-doped tube is energetically favorable. Clearly, if there was carbon feedstock in the vapor phase during the quantum dynamics simulation, it could easily lead to tube closure that includes the N atoms within the lattice. This type of closure would lead to the bell-type structures commonly observed for bamboo tubes.

The formation of fullerene-like structures encapsulated within N-doped nanotubes (Figure 2d) might be partially caused by the fact that small amounts of nitrogen gas can be encapsulated within a tube or intercalated between tube walls. This has been observed experimentally,[35] and some additional support has been obtained from tight-binding calculations,[36] X-ray photoelectron spectroscopy (XPS), and electron-energy-loss spectroscopy (EELS). For tube growth in the presence of N, the tube undergoes N doping and closes (as described above), forming compartments and bamboo-like structures. Both encapsulation of gaseous N and its intercalation (for MWNTs) can occur at this point. The excess N can then undergo secondary chemical reactions with the tube wall near the substitutional N defects where there is enhanced reactivity, causing the formation of smaller fullerene structures that become encapsulated in the growing outside tube (for MWNTs). Simulations based on first-principles molecular dynam-

ics, in which a small N-doped SWNT compartment (two N atoms in the (8,0) SWNT lattice near one end cap) with an encapsulated N molecule was heated to 3500 K over 5 ps, did not show any evidence to support this hypothesis. The N_2 molecule remained inert for that time period. However, if the calculation is carried out with N atoms instead of a N_2 molecule (this assumes that either dissociated N is encapsulated or the molecular N undergoes dissociation after encapsulation), the dynamics leads to the formation of chemical bonds near the N substitutional tube defect, generating pentagons and causing inward bending of the structure toward a defected graphitic dome (see Supporting Information, Figure S2). This process will lead to the formation of two fullerene-like structures and helps explain the origin of the images described above (Figure 2d). It is also possible that fullerene particle formation could occur first and not as a secondary chemical reaction. This could result from a frustrated growth (higher %N should enhance the event), which is then encapsulated by a stable growing tube due to capillary action.

Finally, if N atoms are included into the tube lattice during growth, there is an enhanced chemical reactivity that is likely fundamental to the observation that N-doped tubes tend to oxidize more easily. For example, under appropriate conditions, there can be strong enough interactions between doped tubes to form interconnecting chemical bonds.[37] However, the intertube interaction found by Nevidomskyy *et al.*[37] would require very high levels of doping and high pressure (they estimate 80 GPa to achieve the intertube distance, 2.5 Å, required to form the bond). Instead, if nanotube bundles are held together by van der Waals forces, defective and disordered nanotube walls which result from N doping should weaken the van der Waals forces (disrupting the $\pi-\pi$ interactions) and consequently cause weaker tube−tube interactions. In ref 27, it was shown that, as the nitrogen content is increased, the Raman D-to-G band ratio is also increased, indicating a higher degree of disorder due to the inclusion of the nitrogen atoms into the hexagonal lattice, which is consistent with the corrugated nanotube walls shown in Figure 2e. The latter explains why it is easier to disperse the N-doped NTs compared to pristine NTs (chemical reactivity may also help, since graphene is an inert surface). Confirmation of this result can be seen in Figure 3, which shows that, with increasing doping levels, the entanglement of the nanotubes is reduced, and it is easier to find smaller nanotube bundles and isolated nanotubes. This is consistent with reduced interactions and also with the increased difficulty to collect the sample as doping increases, since the collected strand is more fragile for higher doping levels due to reduced entanglement. In order to verify that N-doped SWNTs have weaker interactions, we computed the tube−tube binding energy for doped (2.0−6.2% N substitution) and pristine (8,0) SWNTs from first-principles

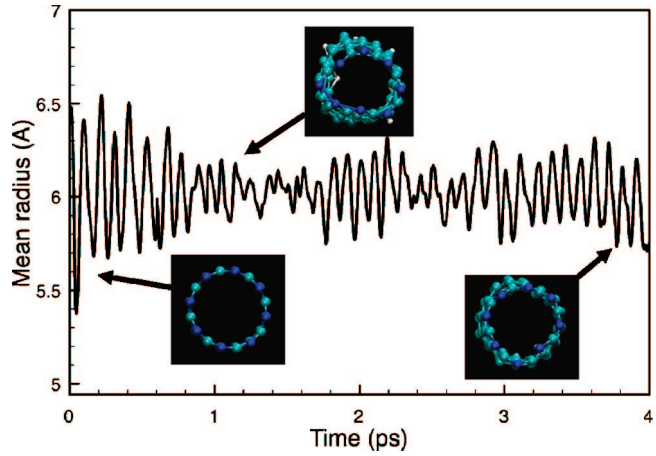

Figure 5. Time dependence of the diameter for a N-doped (8,0) SWNT (top) (N atoms on the rim at the 2-coordinated sites). The results are taken from the first-principles MD simulation at 2500 K. The insets show snapshots of the structure for the N-doped (8,0) SWNT at $T = 0$, 0.163, and 4 ps, taken from the quantum molecular dynamics simulations.

calculations (using DFT/LDA and DFT/GGA revPBE functionals). These calculations reveal that N-doped (substitutional type) tubes have on the order of a 14–30 meV/atom smaller tube−tube interaction (with higher N content giving the weaker interaction), unless the N defects on each tube are directly aligned and the intertube distance becomes small enough (~2.5 Å, even for multiple N sites) to allow the formation of a chemical bond. We also have computed the fracture strength of N-doped SWNTs as compared to pristine SWNTs by computing the deformation required to fracture the tubes (see Supporting Information). These results indicate that N-doped tubes will fracture at half the deformation of that for pristine tubes, in agreement with the above experimental observations of increased fragility.

CONCLUSIONS

In summary, we have demonstrated, using a combination of experimental observations and first-principles static and dynamics calculations, that nitrogen mediates the growth of SWNTs by acting as a surfactant, leading to systems favoring smaller diameters. A good surfactant generally facilitates growth by allowing subsurface insertion of the feedstock material at reduced energetic cost. In that respect, nitrogen appears not to be a great surfactant, since it also was found to promote tube closure, leading to shorter tubes. Tube closure that includes N atoms inside the lattice is also preferred, thereby suggesting that the presence of morphologies such as bamboo structures can be triggered by the presence of N dopants. The inclusion of N inside the tube lattice leads to weaker tube−tube interactions as well as providing sites where encapsulated or intercalated N can undergo chemical reaction, which may form smaller fullerene structures that become encapsulated within the compartment.

MATERIALS AND METHODS

The generation of aligned CN_x ($x < 0.1$) nanotubes is possible using template methods involving porous alumina membranes or laser-etched metal films deposited on silica substrates,[38] by pyrolyzing mixtures of ferrocene and melamine[28] or solutions of ferrocene, ethanol, and benzylamine.[27] Striking features about these types of tubes are their diameter, morphology, and degree of uniformity. In the present work, we examine N-doped single CNTs prepared mainly by using thermal decomposition of mixtures of ferrocene/ethanol/benzylamine, which yields smaller diameter tubes forming long strands of SWNTs,[27] and those from pyrolysis of ferrocene/benzylamine mixtures, which produce MWNTs with corrugated and bamboo-like morphologies.[28,29] The synthesized N-doped CNTs have been carefully characterized by HRTEM, EELS, XPS, TGA, and transport measurements.

All modeling calculations were performed using the periodic DFT program Vienna *ab initio* simulation package (VASP), version 4.6.6.[39–42] The Kohn–Sham equations were solved using the projector augmented wave (PAW) approach[43,44] and a plane-wave basis with a 400 eV energy cutoff. Unless otherwise stated, the generalized gradient approximation (GGA) exchange-correlation functional of Perdew, Burke, and Ernzerhof (PBE)[45] was utilized. Electronic convergence was defined as a consistency between successive cycles of less than 10^{-5} eV. Each nanotube system was placed in a cell that ensured at least 10 Å of vacuum in each Cartesian direction between the tube and its reflection. *k*-point sampling was restricted to a single point, the Γ point, a choice that is relevant for the finite cluster calculations performed here. Note that some care needs to be taken due to the open-shell (dangling bonds) nature of most of the structures studied, as the lowest energy electronic configuration can be one of the higher spin states.

In order to explore the effects of chirality, we first carried out static electronic structure calculations for (9,0), (9,3) and (6,6) SWNTs consisting of 111, 106, and 106 atoms, respectively. For the detailed analysis of N-doping, we studied an (8,0) tube consisting of 104 atoms, including 8 nitrogen and 8 hydrogen atoms. The hydrogen atoms are used to passivate the nanotube end opposite to the growth edge. The energetics relative to the positions of the N atoms in the nanotube lattice was computed from full geometry relaxation as $E_{binding} = [E(\text{N doped with } 2n \text{ N atoms}) - nE(N_2) - E(\text{tube without N atoms})]$, where n is the number of nitrogen molecules needed to form a complete ring of $2n$ N atoms. The effects of temperature on the N-doped CNTs were investigated with first-principles molecular dynamics simulations (1 fs dynamical time step) with a Nosé–Hoover thermostat[46] to regulate the ion temperature to ~2500 K over 5 ps. We also carried out complementary simulations on undoped CNTs under the same conditions. These studies address the role of the N atoms in the dynamic behavior of the tubes at temperatures relevant to the experimental synthesis.

Acknowledgment. This work was supported by the Center for Nanophase Materials Sciences (CNMS), sponsored by the Division of Scientific User Facilities, U.S. Department of Energy, and by the Division of Materials Science and Engineering, U.S. Department of Energy, under Contract No. DEAC05-00OR22725 with UT-Battelle, LLC at Oak Ridge National Laboratory (ORNL). The extensive computations were performed using the resources of the National Center for Computational Sciences at ORNL. This work was also supported in part by CONACYT-México grants [56787 (Laboratory for Nanoscience and Nanotechnology Research-LINAN), 45762 (H.T.), 45772 (M.T.), 41464-Inter American Collaboration (M.T.), 42428-Inter American Collaboration (H.T.), 2004-01-013/SALUD-CONACYT (M.T.), PUE-2004-CO2-9 Fondo Mixto de Puebla (M.T.)] and Ph.D. scholarships (E.C.-S. and J.M.R.-H.), as well as NSF Grant DMR-0303429.

Supporting Information Available: Plot of the energetics associated with the placement of a ring of N atoms in the lattice of a capped (9,0) SWNT, snapshot of the initial stages of fullerene formation taken from quantum MD simulations, and plots of the fracturing of N-doped *versus* pristine nanotubes. This information is available free of charge *via* the Internet at http://pubs.acs.org.

REFERENCES AND NOTES

1. Dresselhaus, M. S.; Dresselhaus, G.; Eklund, P. C. *Science of Fullerenes and Carbon Nanotubes: Their Properties and Applications*; Academic Press: Orlando, FL, 1996.
2. Saito, R.; Dresselhaus, G.; Dresselhaus, M. S. *Physical Properties of Carbon Nanotubes*; Imperial College Press: London, 1998.
3. Charlier, J. C.; Blase, X.; Roche, S. Electronic and Transport Properties of Nanotubes. *Rev. Mod. Phys.* **2007**, *79*, 677–732.
4. Wagner, H. D.; Vaia, R. A. Nanocomposites: Issues at the Interface. *Mater. Today* **2004**, *7*, 38–42.
5. Stephan, O.; Ajayan, P. M.; Colliex, C.; Redlich, P.; Lambert, J. M.; Bernier, P.; Lefin, P. Doping Graphitic and Carbon Nanotube Structures with Boron and Nitrogen. *Science* **1994**, *266*, 1683–1685.
6. Shiraishil, S.; Kibe, M.; Yokoyama, T.; Kurihara, H.; Patel, N.; Oya, A.; Kaburagi, Y.; Hishiyama, Y. Electric Double Layer Capacitance of Multi-Walled Carbon Nanotubes and B−Doping Effect. *Appl. Phys. A: Mater. Sci. Process.* **2006**, *82*, 585–591.
7. Carroll, D. L.; Redlich, P.; Blase, X.; Charlier, J.-C.; Curran, S.; Ajayan, P. M.; Roth, S.; Ruhle, M. Effects of Nanodomain Formation on the Electronic Structure of Doped Carbon Nanotubes. *Phys. Rev. Lett.* **1998**, *81*, 2332–2335.
8. Bernholc, J.; Brenner, D.; Nardelli, M. B.; Meunier, V.; Roland, C. Mechanical and Electrical Properties of Nanotubes. *Annu. Rev. Mater. Res.* **2002**, *32*, 347–375.
9. Yi, J.-Y.; Bernholc, J. Atomic Structure and Doping of Microtubules. *Phys. Rev. B* **1993**, *47*, 1708–1711.
10. Miyamoto, Y.; Cohen, M. L.; Louie, S. G. Theoretical Investigation of Graphitic Carbon Nitride and Possible Tubule Forms. *Solid State Commun.* **1997**, *102*, 605–608.
11. Yang, Q.-H.; Hou, P.-X.; Unno, M.; Yamauchi, S.; Saito, R.; Kyotani, T. Dual Raman Features of Double Coaxial Carbon Nanotubes with N-Doped and B-Doped Multiwalls. *Nano. Lett.* **2005**, *5*, 2465–2469.
12. Endo, M.; Hmuramatsu, H.; Hayashi, T.; Kim, Y. A.; Lier, G. V.; Charlier, J. C.; Terrones, M.; Terrones, H.; Dresselhaus, M. S. Atomic Nanotube Welders: Boron Interstitials Triggering Connections in Double-Walled Carbon Nanotubes. *Nano. Lett.* **2005**, *5*, 1099–1105.
13. Kotakoski, J.; Krasheninnikov, A. V.; Ma, Y.; Foster, A. S.; Nordlund, K.; Nieminen, R. M. B and N Ion Implantation into Carbon Nanotubes: Insight from Atomistic Simulations. *Phys. Rev. B* **2005**, *71*, 205408-1205408-6.
14. Kong, J.; Zhou, C.; Yenilmez, E.; Dai, H. Alkaline Metal-Doped n-Type Semiconducting Nanotubes as Quantum Dots. *Appl. Phys. Lett.* **2000**, *77*, 3977–3979.
15. Jourdain, V.; Stephan, O.; Castignolles, M.; Loiseau, A.; Bernier, P. Controlling the Morphology of Multiwalled Carbon Nanotubes by Sequential Catalytic Growth Induced by Phosphorus. *Adv. Mater.* **2004**, *16*, 447–453.
16. Manna, D. J.; Halls, M. D. Ab initio Simulations of Oxygen Atom Insertion and Substitutional Doping of Carbon Nanotubes. *J. Chem. Phys.* **2002**, *116*, 9014–9020.
17. Fagan, S. B.; Mota, R.; Silva, A. J. R.; Fazzio, A. Substitutional Si Doping in Deformed Carbon Nanotubes. *Nano. Lett.* **2004**, *4*, 975–977.
18. Lafdi, K.; Chin, A.; Ali, N.; Despres, J. F. Cobalt-Doped Nanotubes: Preparation, Texture, and Magnetic Properties. *J. Appl. Phys.* **1996**, *79*, 6007–6009.
19. McGuire, K.; Gothard, N.; Gai, P. L.; Dresselhaus, M. S.; Sumanasekera, G.; Rao, A. M. Synthesis and Raman Characterization of Boron-Doped Single-Walled Carbon Nanotubes. *Carbon* **2005**, *43*, 219–227.

20. Terrones, M.; Grobert, N.; Terrones, H. Synthetic Routes to Nanoscale BxCyNz Architectures. *Carbon* **2002**, *40*, 1665–1684.
21. Terrones, M. Carbon Nanotubes: Synthesis and Properties, Electronic Devices and Other Emerging Applications. *Int. Mater. Rev.* **2004**, *49*, 325–377.
22. Wei, B. Q.; Spolenak, R.; Kohler-Redlich, P.; Ruhle, M.; Arzt, E. Electrical Transport in Pure and Boron-Doped Carbon Nanotubes. *Appl. Phys. Lett.* **1999**, *74*, 3149–3151.
23. Fuentes, G. G.; Borowiak-Palen, E.; Pichler, T.; Liu, X. W.; Graff, A.; Behr, G.; Kalenczuk, R. J.; Knupfer, M.; Fink, J. Electronic Structure of Multiwall Boron Nitride Nanotubes. *Phys. Rev. B* **2003**, *67*, 035429.
24. Xu, W. H.; Kyotani, T.; Pradhan, B. K.; Nakajima, T.; Tomita, A. Synthesis of Aligned Carbon Nanotubes with Double Coaxial Structure of Nitrogen-Doped and Undoped Multiwalls. *Adv. Mater.* **2003**, *15*, 1087–1090.
25. Yang, Q. H.; Xu, W. H.; Tomita, A.; Kyotani, A. Dual Raman Features of Double Coaxial Carbon Nanotubes with N-Doped and B-Doped Multiwalls. *Chem. Mater.* **2005**, *11*, 2940–2469.
26. Blase, X.; Charlier, J.-C.; Vita, A. D.; Car, R.; Redlich, P.; Terrones, M.; Hsu, W. K.; Terrones, H.; Carroll, D. L.; Ajayan, P. M. Boron-Mediated Growth of Long Helicity-Selected Carbon Nanotube. *Phys. Rev. Lett.* **1999**, *83*, 5078–5081.
27. Villalpando-Paez, F.; Zamudio, A.; Elias, A. L.; Son, H.; Barros, E. B.; Chou, S. G.; Kim, Y. A.; Mauramatsu, H.; Hayashi, T.; Kong, J.; et al. Synthesis and Charaterization of Long Strands of Nitrogen-Doped Single-Walled Carbon Nanotubes. *Chem. Phys. Lett.* **2006**, *424*, 345–352.
28. Terrones, M.; Terrones, H.; Grobert, N.; Hsu, W. K.; Zhu, Y. Q.; Hare, J. P.; Kroto, H. W.; Walton, D. R. W.; Zhang, J. P.; Cheetam, A. K. Efficient Route to Large Arrays of CNx Nanofibers by Pyrolysis of Ferrocene/Melamine Mixtures. *Appl. Phys. Lett.* **1999**, *75*, 3932–3934.
29. Terrones, M.; Redlich, P.; Grobert, N.; Trasobares, S.; Hsu, W. K.; Terrones, H.; Zhu, Y. Q.; Hare, J. P.; Reeves, C. L.; Cheetam, A. K.; et al. Carbon Nitride Nanocomposites: Formation of Aligned CxNy Nanofibers. *Adv. Mater.* **1999**, *11*, 655–658.
30. Charlier, J. C.; Blase, X.; De Vita, A.; Car, R. Microscopic Growth Mechanisms for Carbon and Boron-Nitride Nanotubes. *Appl. Phys. A: Mater. Sci. Process.* **1999**, *68*, 267–273.
31. Rodríguez-Manzo, J. A. Magnetism of Carbon Nanostructures and In-Situ TEM Dynamic Transformations of Carbon-Based Nanomaterials. Ph.D. Thesis, 2007.
32. Trasobares, S.; Stephan, C.; Colliex, C.; Hsu, W. K.; Kroto, H. W.; Walton, D. R. W. Compartmentalizaed CNx Nanotubes: Chemistry, Morphology, and Growth. *J. Chem. Phys.* **2002**, *116*, 8966.
33. Ahn, H. S.; Lee, S. C.; Han, S.; Lee, K. R.; Kim, D. Y. Ab Initio Study of the Effect of Nitrogen on Carbon Nanotube Growth. *Nanotechnology* **2006**, *17*, 909–912.
34. Ewels, C. P. Nitrogen Violation of the Isolated Pentagon Rule. *Nano Lett.* **2006**, *6*, 890–895.
35. Terrones, M.; Kamalakaran, R.; Seeger, T.; Ruhle, M. Novel Nanoscale Gas Containers: Encapsulation of N_2 in CNx Nanotubes. *Chem. Commun.* **2000**, *2000*, 2335–2336.
36. Choi, H. C.; Bae, Y.; Park, J.; Seo, K.; Kim, C.; Kim, B.; Song, H. J.; Shin, H.-J. Experimental and Theoretical Studies on the Structure of N-Doped Carbon Nanotubes: Possibility of Intercalated Molecular N_2. *Appl. Phys. Lett.* **2004**, *85*, 5742–5744.
37. Nevidomskyy, A. H.; Casanyi, G.; Payne, M. C. Chemically Active Substitutional Nitrogen Impurity in Carbon Nanotubes. *Phys. Rev. Lett.* **2003**, *91*, 105502-1105502-4.
38. Sung, S. L.; Tsai, S. H.; Tseng, C. H.; Chiang, F. K.; Liu, X. W.; Shih, H. C. Well-Aligned Carbon Nitride Nanotubes Synthesized in Anodic Alumina by Electron Cyclotron Resonance Chemical Vapor Deposition. *Appl. Phys. Lett.* **1999**, *74*, 197–199.
39. Kresse, G.; Hafner, G. Ab Initio Molecular Dynamics for Liquid Metals. *Phys. Rev. B* **1993**, *47*, 558–561.
40. Kresse, G.; Hafner, J. Ab Initio Molecular-Dynamics Simulation of the Liquid-Metal-Amorphous-Semiconductor Transition in Germanium. *Phys. Rev. B* **1994**, *49*, 14251–14269.
41. Kresse, G.; Furthmuller, J. Efficiency of Ab-Initio Total Energy Calculations for Metals and Semiconductors Using a Plane-Wave Basis Set. *Comput. Mater. Sci.* **1996**, *6*, 15–50.
42. Kresse, G.; Furthmuller, J. Efficient Iterative Schemes for Ab Initio Total-Energy Calculations Using a Plane-Wave Basis Set. *Phys. Rev. B* **1996**, *54*, 11169–11186.
43. Kresse, G.; Joubert, D. From Ultrasoft Pseudopotentials to the Projector Augmented-Wave. *Methods Phys. Rev. B* **1999**, *59*, 1758–1775.
44. Blochl, P. E. Projector Augmented-Wave Method. *Phys. Rev. B* **1994**, *50*, 17953–17979.
45. Perdew, J. P.; Burke, K.; Ernzerhof, M. Generalized Gradient Approximation Made Simple. *Phys. Rev. Lett.* **1996**, *77*, 3865–3868.
46. Nosé, S. A Unified Formulation of the Constant Temperature Molecular Dynamics Methods. *J. Chem. Phys.* **1984**, *81*, 511–519.